

A Monolithic Ge-on-Si CMOS Imager for Short Wave Infrared

B. Ackland, C. Rafferty, C. King, I. Aberg, J. O'Neill, T. Sriram, A. Lattes, C. Godek and S. Pappas.

NoblePeak Vision

500 Edgewater Dr., Ste 570, Wakefield MA 01880. USA.

Ph: +1(781) 224-9740 email: bbackland@noblepeak.com

Introduction

Imaging in the Short Wave Infrared (SWIR) band (1-2 μm) enables a broad range of applications in medical and dental imaging, industrial inspection and night vision. The night sky emits substantially more light in this band than in the visible. The spectral response of silicon detectors is limited to $\lambda < \sim 1\mu\text{m}$. SWIR imagers have traditionally been built using arrays of compound semiconductor detectors hybridized to a silicon read-out circuit but are prohibitively expensive for many applications. Germanium is chemically compatible with silicon and optically responsive from blue to 1.6 μm but until now, there has been no good technique for integrating single-crystal germanium detectors on silicon. This paper describes a monolithic CMOS imager with Ge detectors fabricated within a conventional 180 nm CMOS foundry process.

Night Sky

The light from a clear moonless sky is dominated by night glow, also known as ‘‘airglow’’, caused by various processes in the upper atmosphere, including cosmic rays and chemical luminescence caused by hydroxyl ions at high altitude [1]. The spectral distribution of the night sky is as follows [2]:

Wavelength (λ)	Photons (/cm ² /s)
0.4-0.7 μm (visible)	7×10^8
0.4-1.0 μm (Si)	3×10^9
0.4-1.4 μm	2.5×10^{10}
0.4-2.0 μm	1×10^{11}

The 35-fold increase in available light between visible and 1.4 μm presents an opportunity for passive night vision. A fast lens can deliver 3×10^9 of the available photons in the 0.4-1.4 μm band to the imager faceplate. At a 10 μm pixel pitch and 30 fps operation, this translates to 100 photons per pixel per frame. Sensitivity in the band $\lambda=1.4\text{-}2.0 \mu\text{m}$ provides another potential 300 photons, depending on cutoff wavelength.

To take advantage of the available photon supply, low noise (preferably single digit electrons) and high quantum efficiency up to at least $\lambda=1.4 \mu\text{m}$ are required. Silicon detectors have outstanding noise performance, but only generate ~ 1 electron of signal under the above conditions.

Device and Process Technology

Germanium is an excellent detector candidate, with a cutoff wavelength $\sim 1600 \text{ nm}$ [3] and widespread use in CMOS production [4] [5] Germanium has the same lattice structure as silicon, and alloys of any composition may be

formed with silicon. Ge can be ion implanted and annealed at low temperature. Figure 1 shows the absorption rate of light for Si, Ge and InGaAs detectors. Absorption in Ge is higher than Si even in the visible and continues out to 1.6 μm . Ge has been grown on silicon, e.g. [6] [7], but the lattice mismatch between Ge and Si has hitherto prevented integrating high quality Ge detectors with CMOS. Detectors need to be *thick*, *pure* and *defect-free* to achieve the necessary dark current and quantum efficiency.

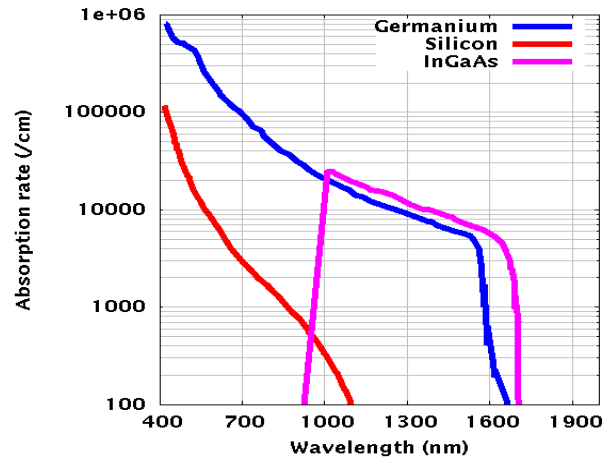


Figure 1 – Absorption in Si, Ge and InGaAs

Figure 2 shows schematically our growth technique [8] [9] which traps dislocations by exploiting their characteristic diagonal propagation. A single crystal seed emerges from the narrow aperture and serves as a crystalline template for a large defect-free island. The island is formed after silicon transistor formation. The conventional back-end of the CMOS process then proceeds as usual, with alternating layers of dielectric and metal used to interconnect transistors and to connect the germanium photodiode to the circuitry.

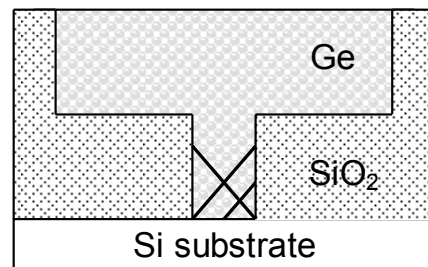


Figure 2 – Germanium selective growth

Figure 3 shows a scanning electron micrograph (SEM) of one such island integrated into a 180 nm CMOS process with three levels of metal and a reflow microlens.

Detectors of size from 2 μm to 5.6 μm and imaging arrays with pixels of size 7 μm and 10 μm have been fabricated in this technology.



Figure 3 – Germanium diode embedded in CMOS

The detector anode and cathode are formed by ion implantation, allowing the use of a lateral diode structure. The junction area, the main source of dark current, is $\sim 1\%$ of the photon-collecting area. This is in contrast to the grown-in vertical diode structure usually found in compound semiconductor infrared detectors, where the main sources of photo-current and dark current necessarily have the same area. For the same reason, the detector capacitance is low, at less than 10 fF. The dark current is significantly higher than silicon due to the smaller bandgap of germanium. Presently, the dark current is dominated by non-ideal generation-recombination current at the junction surface due to imperfect dielectric passivation, and cooling is required. Process and device improvements are under way to mitigate G-R currents and transition to the diffusion limit, less than 1 nA/cm^2 at room temperature in our structure.

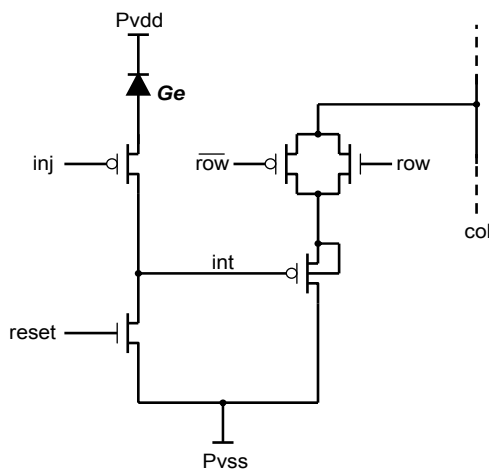


Figure 4 – Pixel circuit

Circuit Design

The imager uses a 5-T injection pixel as shown in Figure 4. Although the imager detector is only $4 \times 4 \mu\text{m}$, we use a $10 \mu\text{m}$ pixel in conjunction with a microlens to provide sufficient light gathering for night vision applications. This extra space allows us to use a relatively large bootstrapped PMOS source follower. The increased size of this device provides a reduction in $1/f$ noise. The bootstrapping provides improved gain and linearity along with substantially reduced integration capacitance. An NMOS reset transistor provides increased dynamic range and reduced “twinkling” [10] due to the minimal stress on the transistor drain under reset conditions. An injection transistor maintains a low bias on the detector (to minimize dark current), increased dynamic range and also isolates the detector capacitance from the integration node, achieving a conversion gain of $40 \mu\text{V/e}$. Pixel output is provided via a complementary pass gate to exploit the extended dynamic range of the pixel.

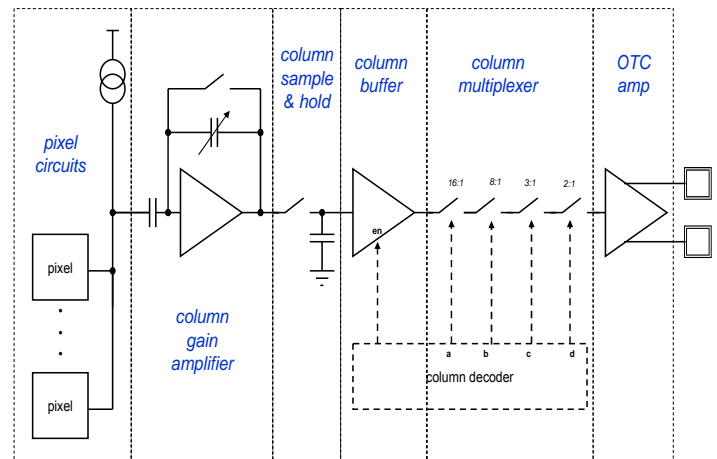


Figure 5 – Analog signal chain

Pixels are reset and read-out on a row-by-row basis using a conventional “rolling shutter” with programmable integration time. Each column (Figure 5) includes a variable gain (0.5x to 8x) switched capacitor amplifier that provides analog correlated double sampling (CDS) to remove pixel offset and $1/f$ noise. The pixel source follower/column amplifier combination achieves a dynamic read noise of less than $5e^-$. A sample & hold and 4-stage column multiplexer convert pixel outputs into an analog serial stream. The sample & hold buffer amplifiers, which must drive the capacitance of the column decoder, are enabled by the column decoder to reduce power dissipation. A complementary open-drain current mode output amplifier provides high speed, low power, low pin-out and low noise. A pair of off-chip transimpedance amplifiers and a 12-bit A/D convert the current mode outputs to a digital value. Each pixel is read-out twice per frame: once at the beginning and then at the end of the integration cycle to provide a second stage of digital CDS which removes pixel kT/C noise. Pixel dark signal and

column fixed pattern noise are removed using dark frame subtraction. A digital control block provides programmable timing and pixel addressing and also sets analog bias parameters via a number of on-chip D/A's.

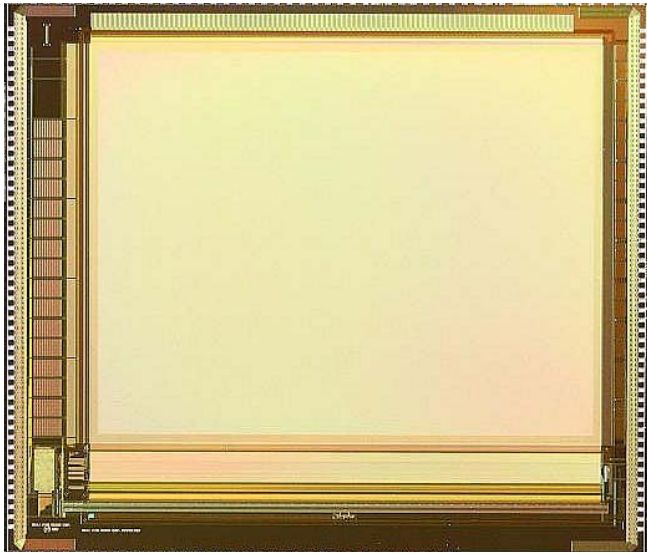


Figure 6 - Chip photomicrograph

Fabrication and Packaging

A 768x600 visible-to-SWIR imager, TriWave[®], designed to support NTSC, PAL and digital VGA up to 30 frames/sec has been fabricated using a commercially available 3M/1P 180 nm foundry process enhanced with Ge photodiodes. Figure 6 shows a photomicrograph of the imager. Crosstalk between the digital and analog sections of the imager is minimized using a combination of deep n-well isolation, guard rings and separate analog and digital I/O blocks. The chip is packaged in a telecom style butterfly package with an integrated thermoelectric cooler (TEC) as shown in Figure 7. The chip design is optimized for low pin-out and low dissipation (<40 mW) in order to minimize the thermal load on the TEC. The TEC can provide cooling down to -90°C, but in normal operation cools to -70°C using under 10W of power.

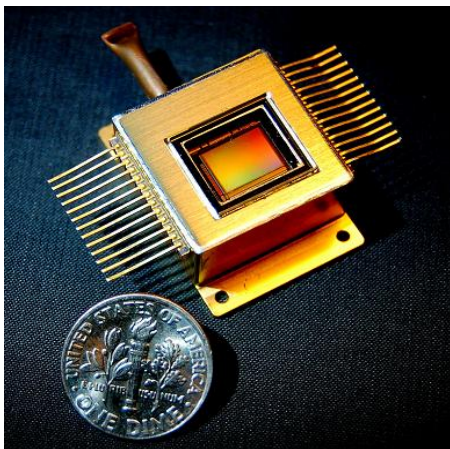


Figure 7 - Packaged TriWave[®] Imager

Results

Figure 8 shows the tradeoff in read noise vs. dynamic range of the readout circuitry for two different values of column gain. Measured signal and noise are plotted as a function of integration time at constant illumination. At a column gain of 4x, the read noise is only 5e-, but the dynamic range (DNR) of the readout circuitry is limited to about 55dB. At a gain of 0.5x, the read noise increases to 17e-, but the DNR extends to 68dB. Note that under saturation, the digital CDS no longer cancels the 27 e- of kT/C noise that is present in the reset image.

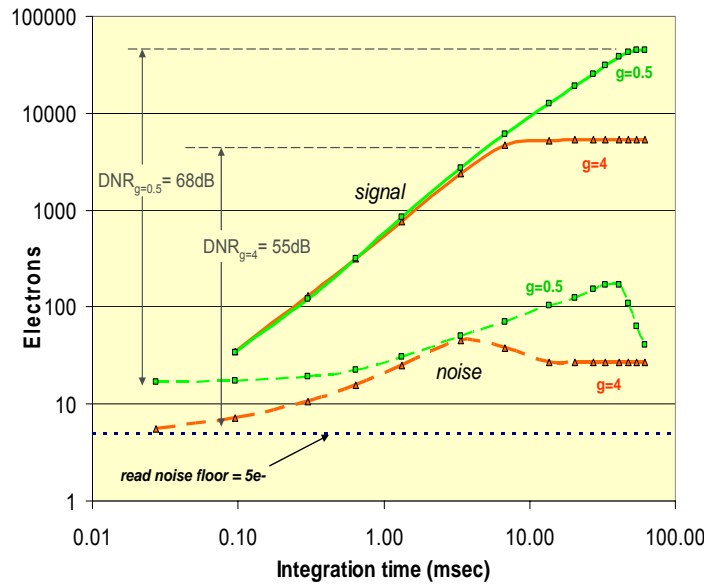


Figure 8 - Readout signal & noise

Figure 9 shows the measured spectral response compared to theoretical predictions for bulk germanium at 220K. The cut off is at longer wavelength than predicted, due to grown-in strain [11] Figure 10 shows the sensitivity of the imager at 1300nm at normal and reduced frame rates. The noise-equivalent illumination at 3.75 fps is 0.52 nW/cm².

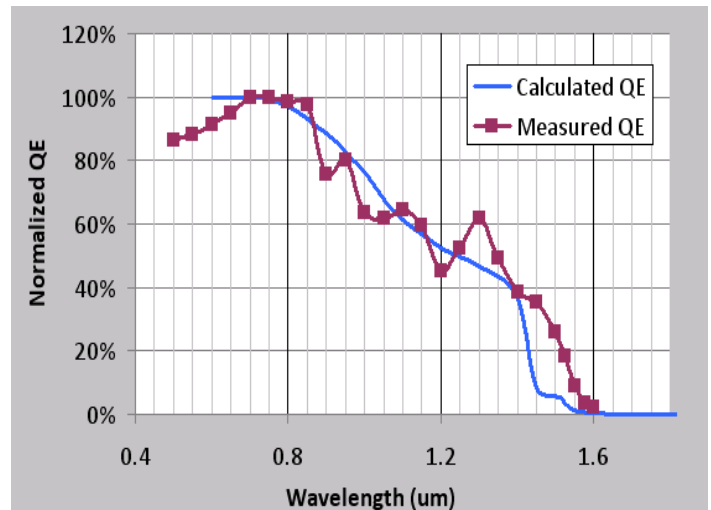


Figure 9 - Normalized spectral response

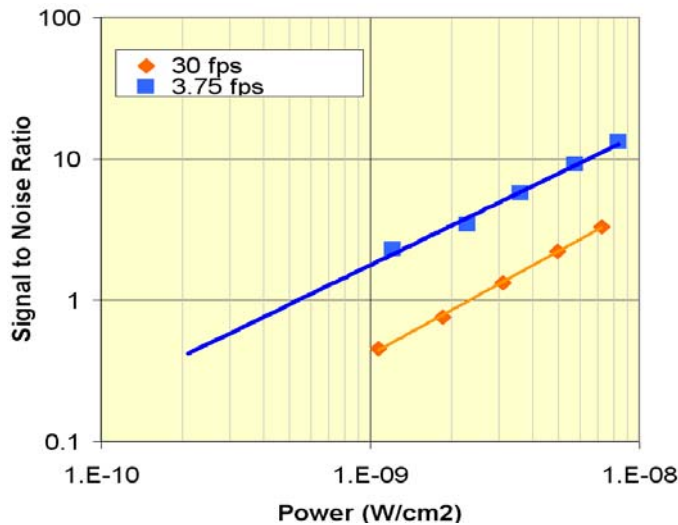


Figure 10 - Imager sensitivity

Dark current and optical response distributions are shown in Figure 11. Pixel yield is greater than 98% and 90% of the pixels have optical response within +/- 16% of the median. Sample day-time (visible light) and night-time moonless (SWIR) images are shown in Figures 12 and 13. Future work will focus on increasing night-time SNR

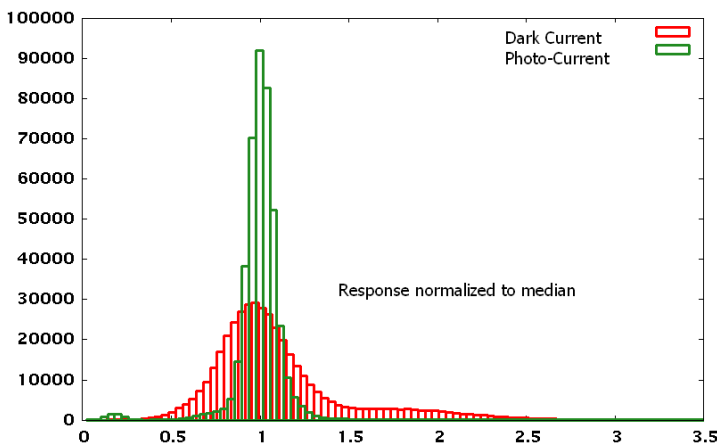


Figure 11 - Dark current and photo-response uniformity



Figure 12 - Rainy Day Image

through a combination of reduced dark current, increased quantum efficiency, larger and thicker detectors and improved broad spectrum microlens design.



Figure 13 - Moonless night image

References

- [1] <http://en.wikipedia.org/wiki/Airglow>
- [2] W.E. Tennant, S. Cabelli, and K. Spariosu, "Prospects of Uncooled HgCdTe Detector Technology", Journal of Electronic Materials, Vol. 28, No. 6, p.582 (1999)
- [3] W.C. Dash, R. Newman, "Intrinsic Optical Absorption in Single-Crystal Germanium and Silicon at 77K and 300K", Physical Review Vol. 99(4), p 1151 (1955)
- [4] D. Lammers, "High-k, strained Si leaving the lab", Electrical Engineering Times 09/29/2003
- [5] C-H. Jan et al, "A 65 nm Ultra Low Power Logic Platform Technology using Uni-axial Strained Silicon Transistors", Proceedings of the IEEE International Electron Device Meeting, p65 (2005)
- [6] L. Colace, G. Masini, V. Cencelli, F. DeNotaristefani, and G. Assanto, IEEE Journal of Quantum Electronics, "A Near-Infrared Digital Camera in Polycrystalline Germanium Integrated on Silicon", Vol. 43(4), p. 311 (2007)
- [7] Y.Kang et al, "Monolithic germanium/silicon avalanche photodiodes with 340 GHz gain-bandwidth product", Nature Photonics Online, 7 Dec 2008
- [8] C.A. King, C.S. Rafferty, US Patent 7,453,129, "Image sensor comprising isolated germanium photodetectors integrated with a silicon substrate and silicon circuitry"
- [9] J.D. Bude, C.A. King, M.S. Carroll, US Patent 7,012,314, "Semiconductor devices with reduced active region defects and unique contacting schemes"
- [10] B. Pain, T. Cunningham, B. Hancock, C. Sun and C. Wrigley, "Twinkling Pixels: Random Telegraph Signals at Reset Gate Edge", Proc. International Image Sensor Workshop, June 2007, pp. 234-237.
- [11] Y. Ishikawa, K. Wada, D. Cannon, J. Liu, H.-C. Luan, L. Kimerling, "Strain-induced band gap shrinkage in Ge grown on Si substrate", Applied Physics Letters Vol 82(13) p. 2044 (2003)